Faraday Discussions

Accepted Manuscript

This manuscript will be presented and discussed at a forthcoming Faraday Discussion meeting. All delegates can contribute to the discussion which will be included in the final volume.

Register now to attend! Full details of all upcoming meetings: http://rsc.li/fd-upcoming-meetings

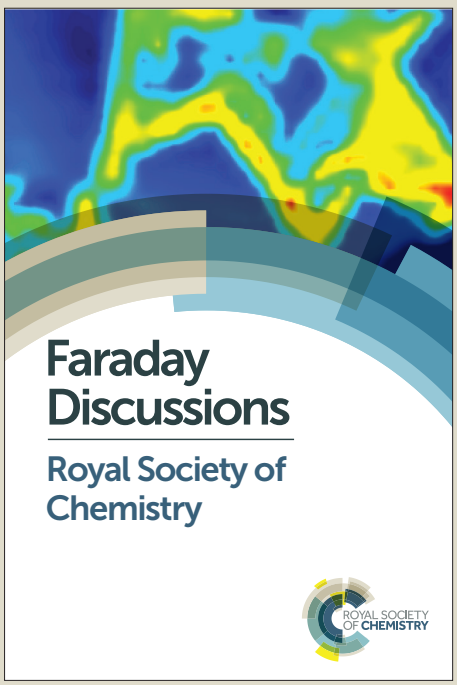

This is an *Accepted Manuscript*, which has been through the Royal Society of Chemistry peer review process and has been accepted for publication.

Accepted Manuscripts are published online shortly after acceptance, before technical editing, formatting and proof reading. Using this free service, authors can make their results available to the community, in citable form, before we publish the edited article. We will replace this *Accepted Manuscript* with the edited and formatted *Advance Article* as soon as it is available.

You can find more information about *Accepted Manuscripts* in the Information for Authors.

Please note that technical editing may introduce minor changes to the text and/or graphics, which may alter content. The journal's standard Terms & Conditions and the Ethical guidelines still apply. In no event shall the Royal Society of Chemistry be held responsible for any errors or omissions in this *Accepted Manuscript* or any consequences arising from the use of any information it contains.

ROYAL SOCIETY OF CHEMISTRY

www.rsc.org/faraday_d

Highly luminescent gold nanoparticles: effect of ruthenium distance for nanoprobes with enhanced lifetimes

Shani A. M. Osborne and Zoe Pikramenou*

School of Chemistry, University of Birmingham, Edgbaston, Birmingham, B15 2TT, United Kingdom.

Abstract

The photophysical properties of gold nanoparticles, AuNP, with sizes of 13, 50 and 100 nm in diameter, coated with surface-active ruthenium complexes have been studied to investigate the effect of distance of the ruthenium luminescent centre from the gold surface. Luminescence lifetimes of three ruthenium probes, RuS1, RuS6 and RuS12, with different length spacer unit between the surface active groups and the ruthenium centre were taken. The metal complexes were attached to AuNP13, AuNP50 and AuNP100 via thiol groups using a method of precoating the nanoparticles with a fluorinated surfactant. The luminescence lifetime of the longer spacer unit complex, RuS12, was enhanced by 70% upon attachment to the AuNP when compared to the increase of the short and medium linker unit complexes, RuS1 (20%) and RuS6 (40%) respectively. The effect of the surfactant in the lifetime increase of the ruthenium coated AuNP was shown to be larger for the medium spacer probe, RuS6. There was no effect of the change of the size of the AuNP from 13 to 50 or 100 nm.

Introduction

Gold nanoparticles, AuNP, are ideal probes for cellular imaging based on their high electron density, which allows multimodal imaging microscopies to be used and improved spatial resolution in detection as opposed to molecular probes. Although the labelling of AuNP with luminescent probes has been reported for some time, a limitation of their use has been the quenching of the molecular fluorescence by different mechanisms involving the surface plasmon of the gold.[1-3]

The distance of the fluorophore to the gold surface and method of attachment are important factors to the luminescent properties of the particles and their studies can provide an understanding of the mechanism involved in quenching of the fluorescence as well as can direct future molecular designs. The quenching of the fluorescence signal by plasmonic nanoparticles in short distances has been attributed to "near-field" effect involving energy or electron transfer non-radiative pathways.[4, 5] In most cases it is shown that if the fluorophore is within 5 nm from the AuNP surface, it is close enough to electronically interact with the AuNP and the fluorophore's excited electron is donated to the gold.[1, 6] More recently, elegant approaches to examine the effect have involved methods for distancing the

fluorophore from the gold surface either through an electrolyte film,[7] using Layer by Layer assemblies,[8] or through formation of silica shells around the gold.[9-11] In many cases it has been shown that organic dyes' fluorescence can be enhanced with increasing the distance from the AuNP, but only achieve lifetimes between the regions of a few ps to 50 ns[12] or 8-fold overall fluorescence enhancement.[8]

We have been interested in the attachment of metal complexes on AuNP to introduce nanoprobes which bear the distinct optical signature of the metal complex, including large Stokes shift and high photostability. Luminescent europium coated AuNP have been prepared and employed as cellular probes.[13-15] To stabilise positively charged ruthenium polypyridyl coated nanoparticles we have used a fluorinated surfactant which has provided a method to stabilise ruthenium luminescent nanoparticles of sizes up to 100 nm.[16] Enhancement of a NIR organic dye has been shown in a system of gold nanorods with silica shells of 17 nm.[11]

It has been shown that the luminescence of ruthenium complexes is quenched when attached to AuNP.[17-19] Adsorption of $Ru(bpy)_3Cl_2$ on the surface of 10 nm AuNP has shown a luminescence lifetime decrease from 623 to 0.8 ns.[6] It was found that even at a distance of 2 nm from the gold surface, a tris(bipyridine)ruthenium complex has a highly quenched luminescence lifetime and an enhancement of 4-fold was seen at a distance of 50 nm via a silica shell.[20]

In our approach the fluorosurfactant coating of the particles has shown to have an effect of protecting the ruthenium probe excited state from quenching by oxygen, increasing the lifetime of the complex on the nanoparticles. The use of surfactant has become increasingly popular for increased stability of nanoprobes.[21] In this study we examine the effect of the luminescence of the ruthenium probe by varying the distance of the attachment of the probe to the surface of the AuNP. We used three ruthenium probes, RuS1, RuS6 and RuS12 (Figure 1), with different length spacer unit between the surface active groups, previously developed in our group.[16, 22, 23] We have also varied the size of the AuNP to examine if there is an influence on the luminescence lifetime of the probes. We describe herein an improved method for coating AuNP using fluorosurfactant stabilised AuNP before ruthenium complex addition. In this study we establish the effect of the length spacer together with the fluorosurfactant interactions for the development of the most efficient design for the ruthenium luminescent nanoparticles.

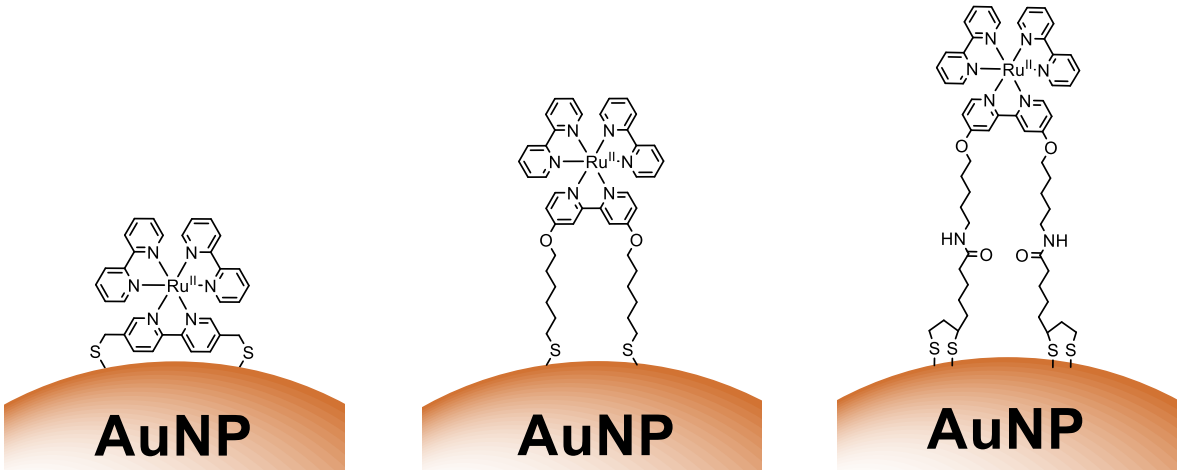

RuS1·AuNP13 **RuS6·AuNP13** **RuS12·AuNP13**

RuS1·AuNP50 **RuS6·AuNP50** **RuS12·AuNP50**

RuS1·AuNP100 **RuS6·AuNP100** **RuS12·AuNP100**

Figure 1: Schematic to show the structure of RuS1·AuNP13, RuS1·AuNP50, RuS1·AuNP100, RuS6·AuNP13, RuS6·AuNP50, RuS6·AuNP100, RuS12·AuNP13, RuS12·AuNP50 and RuS12·AuNP100.

Results and discussion

Gold nanoparticle coating with surfactant and metal complex

Three ruthenium complexes with different sized linker units, RuS1, RuS6 and RuS12 (Figure 1) for the attachment to gold were synthesised and fully characterised following previously published methods.[16, 22, 23] For each complex ion exchange was used to convert the counter ion to chloride, for improved solubility in aqueous solutions, employed in the nanoparticle preparation.

Monodispersed 13, 50 and 100 nm AuNP (AuNP13, AuNP50 and AuNP100) were synthesised using slight modifications of previously published methods.[24-26] The protocol involves synthesising AuNP13 seeds and stabilising with citrate anions. The AuNP were characterised by the specific surface plasmon resonance (SPR) band in visible, transmission electron microscopy (TEM), dynamic light scattering (DLS) sizing and zeta potential measurements (Supplementary Information).

Solutions of AuNP13, AuNP50 and AuNP100 displayed a band with a maximum, λ_{max}, at 517, 532 and 566 nm respectively, characteristic of their SPR band and in agreement with previously published data.[27, 28] DLS sizing confirmed the AuNP13, AuNP50 and AuNP100 to be 14 ± 4 nm (PDI = 0.09), 50 ± 12 nm (PDI = 0.04) and 100 ± 24 nm (PDI = 0.01) respectively. TEM images suggested the sizes of AuNP13, AuNP50 and AuNP100 to be 17, 60 and 120 nm respectively (Supplementary Information) in good agreement with DLS data.

Upon addition of the Zonyl surfactant to the AuNP, a shift of 1 nm of the SPR band is observed. The surfactant coated particles Z·AuNP13 were isolated by centrifugation and they were then used for the titration of the ruthenium probe, monitoring the SPR band (Figure 2).[16]

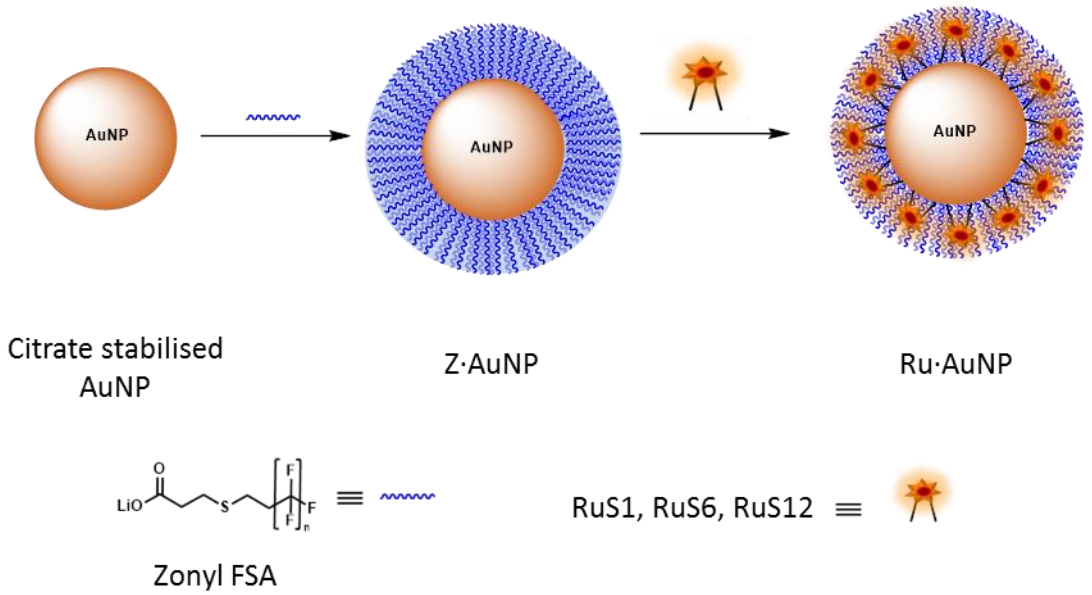

Figure 2: Schematic to show the attachment of fluorinated surfactant, Zonyl FSA, and ruthenium complex to AuNP

For the coating of Z·AuNP13, aliquots (2 µL) of 1.19 mM RuS1, 0.95 mM RuS6 and 0.87 mM RuS12 were titrated into a 4.5 nM solution of Z·AuNP13 and the SPR shift was monitored by the change in λ_{max} to determine the saturation of the AuNP surface (Figure 3). As more probe was added, the SPR shifts to the red until optimum coating is achieved and a shift is no longer observed. Addition of 12 µL 1.19 mM RuS1, 16 µL 0.95 mM RuS6 and 20 µL 0.87 mM RuS12 to 4.5 nM Z·AuNP13 result in a 4 (521 nm), 5 (522 nm) and 3 nm (520 nm) shift in λ_{max} respectively (Table 1). All three probes cause a similar shift in the SPR band upon addition to the AuNP. Analyses of the elemental composition of the nanoparticles by inductively coupled plasma mass spectrometry (ICP-MS) reveal a Ru:Au ratio of 1:160, suggesting coating of 600 ruthenium complexes per AuNP13.

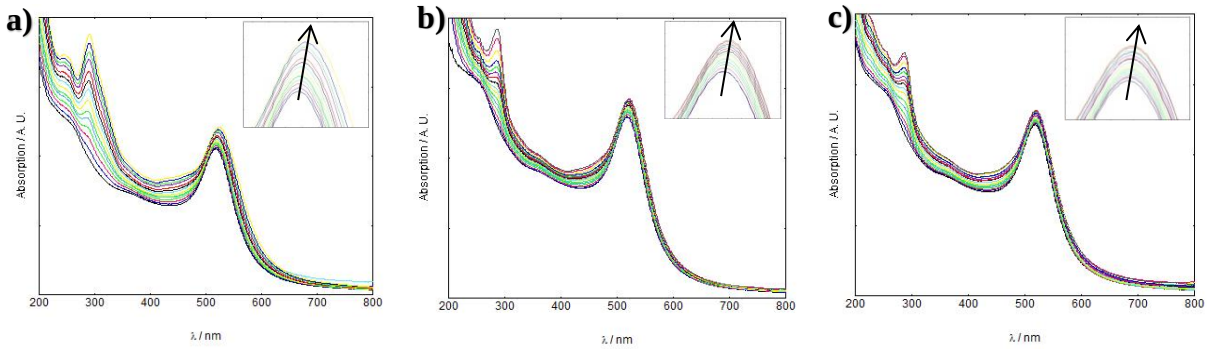

Figure 3: UV-Vis titration of 1.19 mM RuS1 (a), 0.95 mM RuS6 (b) and 0.87 mM RuS12 (c) into 4.5 nM Z·AuNP13 in water.

Table 1: Summary of 13, 50 and 100 nm AuNP SPR shifts upon attachment of Zonyl, RuS1, RuS6 and RuS12.

	λ_{max} (nm)	Shift (nm)		λ_{max} (nm)	Shift (nm)		λ_{max} (nm)	Shift (nm)
AuNP13	517	0	**AuNP50**	532	0	**AuNP100**	566	0
Z·AuNP13	518	1	**Z·AuNP50**	533	1	**Z·AuNP100**	567	1
RuS1·AuNP13	521	4	**RuS1·AuNP50**	537	5	**RuS1·AuNP100**	569	3
RuS6·AuNP13	522	5	**RuS6·AuNP50**	536	4	**RuS6·AuNP100**	569	3
RuS12·AuNP13	520	3	**RuS12·AuNP50**	537	5	**RuS12·AuNP100**	569	3

The particles isolated following size exclusion chromatography showed the same λ_{max} (Figure 4) as the particles saturated with the ruthenium complex, formed during titration. This confirmed that the surface coating of the particles had not changed and only the excess molecular complex was removed during chromatography.

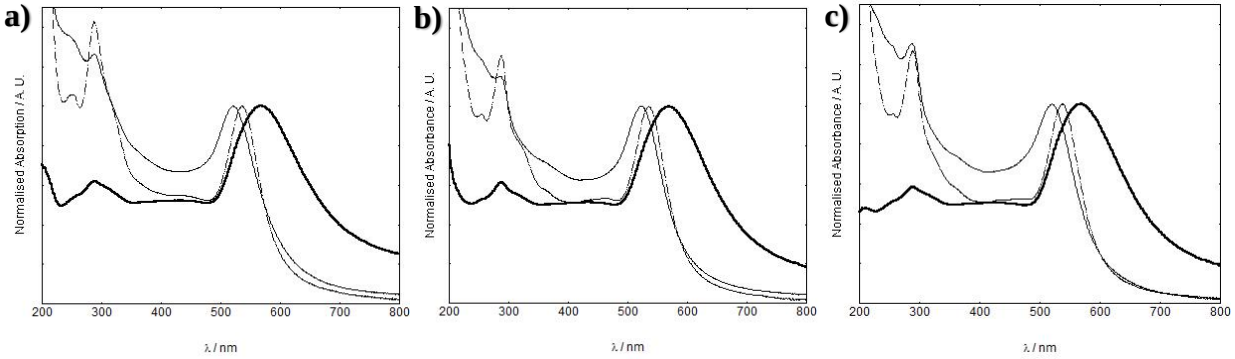

Figure 4: UV-Vis spectra of 4.5 nM RuS1·AuNP13 (thin solid line), 40 pM RuS1·AuNP50 (dotted line) and 20pM RuS1·AuNP100 (thick solid line) (a), 4.5 nM RuS6·AuNP13, 40 pM RuS6·AuNP50 and 20 pM RuS6·AuNP100 (b) and 4.5 nM RuS12·AuNP13, 40 pM RuS12·AuNP50 and 20 pM RuS12·AuNP100 (c) in water.

TEM and DLS studies show that the sizes of the AuNP have not significantly changed upon coating with the surfactant and the ruthenium complex. Images of the nanoparticles by TEM show monodispersed, uniform NPs with estimated sizes from the image of 17 nm for RuS1·AuNP13,

RuS·AuNP13 and RuS12·AuNP13, 60 nm for RuS1·AuNP50, RuS6·AuNP50 and RuS12·AuNP50 and 120 nm for RuS1·AuNP100, RuS6·AuNP100 and RuS12·AuNP100 (Figure 5). The RuS12·AuNP100 were imaged as single nanoparticles by NanoSight tracking both through scatter and ruthenium emission detection in the red upon 488 nm excitation (Supplementary Information).

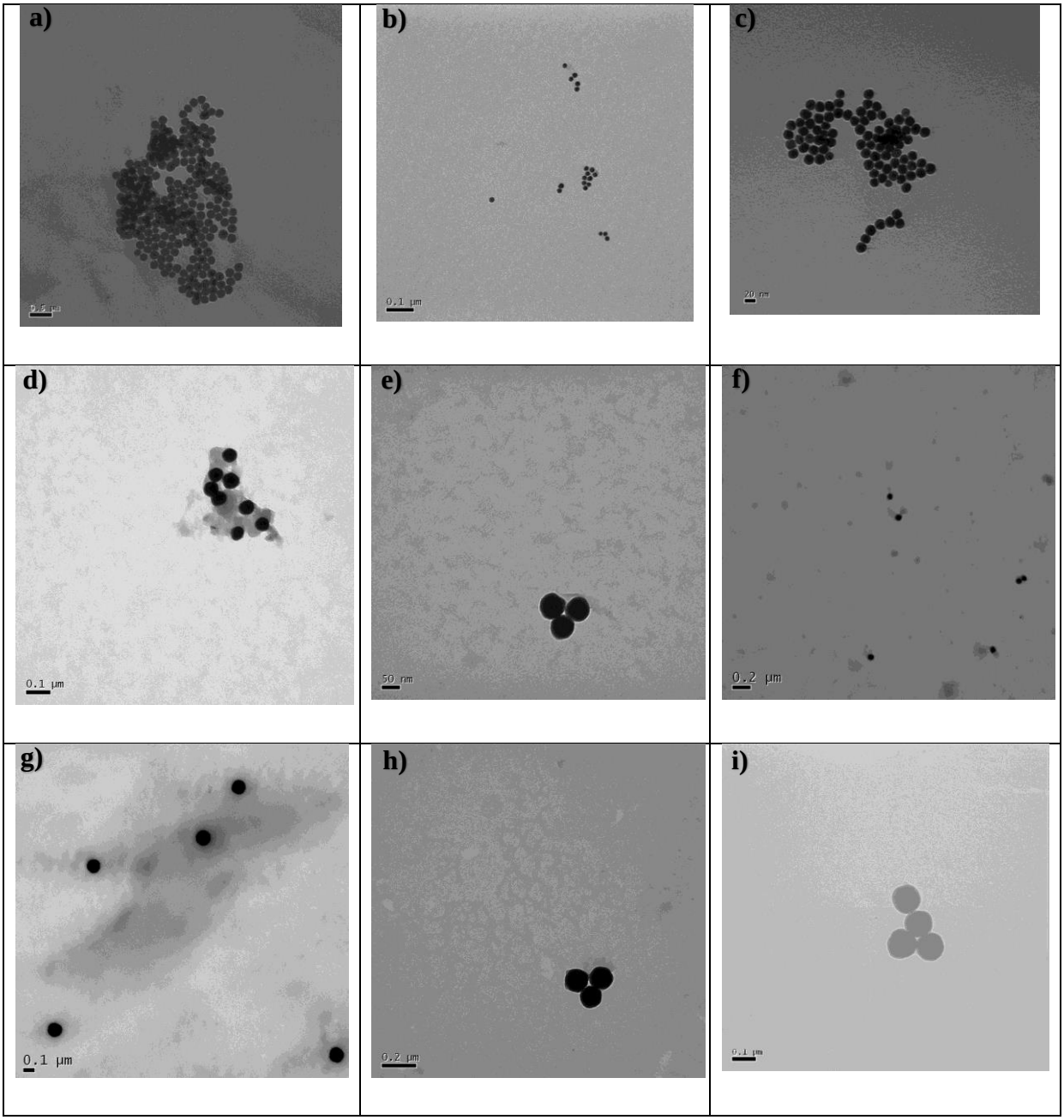

Figure 5: TEM images of RuS1·AuNP13 (a), RuS6·AuNP13 (b), RuS12·AuNP13 (c), RuS1·AuNP50 (d), RuS6·AuNP50 (e), RuS12·AuNP50 (f), RuS1·AuNP100 (g), RuS6·AuNP100 (h) and RuS12·AuNP100 (i). Images are taken on the Jeol 1200 EX TEM.

Luminescent studies of ruthenium probe functionalised AuNP

To characterise the luminescence properties of the probes attached to AuNP, we used steady state and time-resolved emission spectroscopy. The luminescence spectra and lifetime of the nanoprobes were recorded and compared with the molecular complexes in solution, in the presence and absence of the Zonyl surfactant (Figure 6). There is no significant shift in λ_{max} of the emission peak upon addition of Zonyl to the complex or upon attachment of the complex to the Z·AuNP. We have previously found that attachment to a gold surface of the RuS12 complex causes a 15 nm blue shift in λ_{max}.[22] This shift may not be present on the AuNP due to the presence of the surfactant or the different probe environment on the gold surface as compared with the nanoparticle.

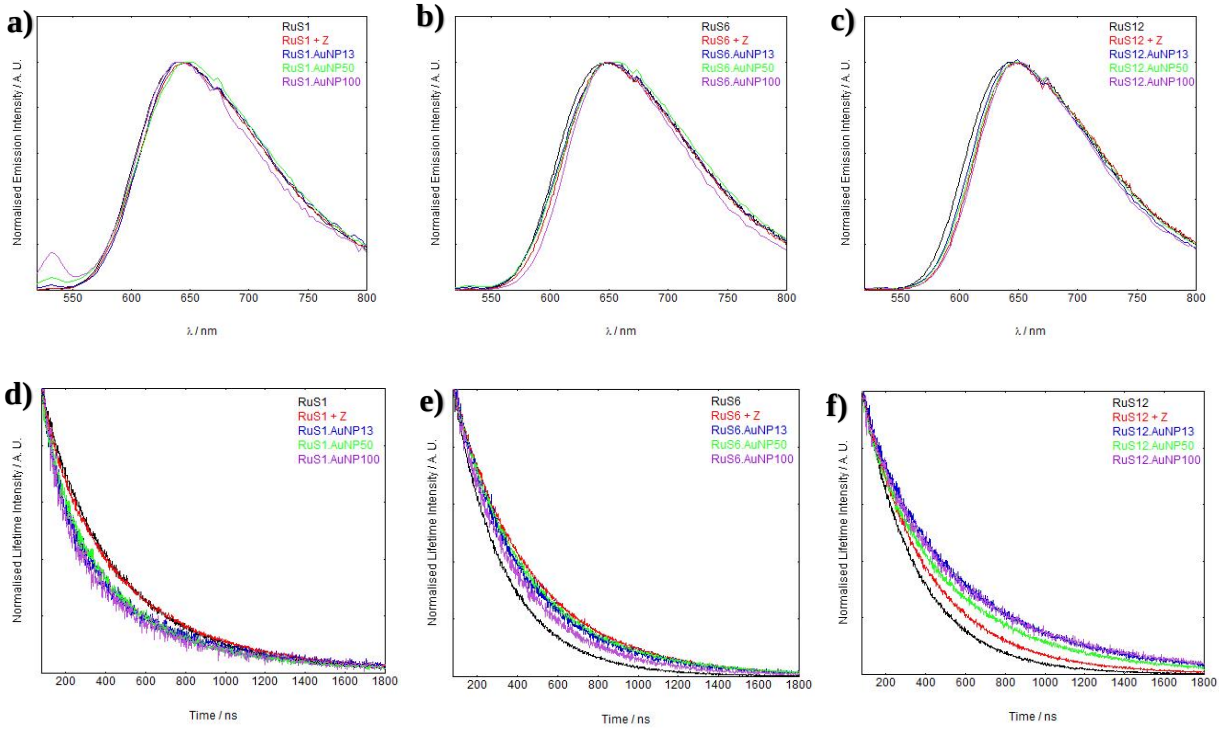

Figure 6: Luminescence emission data of RuS1, RuS1·Z, RuS1·AuNP13, RuS1·AuNP50 and RuS1·AuNP100 (a), RuS6, RuS6·Z, RuS6·AuNP13, RuS6·AuNP50 and RuS6·AuNP100 (b) RuS12, RuS12·Z, RuS12·AuNP13, RuS12·AuNP50 and RuS12·AuNP100 (c). λ_{exc} = 450 nm and λ_{det} = 650 nm. The spectra are taken from 520 – 800 nm. Luminescence lifetime data of RuS1, RuS1 + Z, RuS1·AuNP13, RuS1·AuNP50 and RuS1·AuNP100 (d), RuS6, RuS6 + Z, RuS6·AuNP13, RuS6·AuNP50 and RuS6·AuNP100 (e) RuS12, RuS12 + Z, RuS12·AuNP13, RuS12·AuNP50 and RuS12·AuNP100 (f). λ_{exc} = 445 nm and λ_{det} = 650 nm.

The luminescence lifetimes of the coated AuNP are summarised in Table 2 and comparison of the lifetime decays are presented to illustrate the changes in the lifetimes (Figure 6).

Table 2: Luminescence lifetimes of the three probes on AuNP and the percentage change in lifetime compared to the free probe in water. The luminescent lifetimes were fitted with a X^2 between 1.0 and 1.2.

	τ /ns	%		τ /ns	%		τ /ns	%
RuS1	420	0	**RuS6**	240	0	**RuS12**	280	0
RuS1 + Z	420	0	**RuS6 + Z**	400	70	**RuS12 + Z**	350	25
RuS1·AuNP13	470	20	**RuS6·AuNP13**	340	40	**RuS12·AuNP13**	480	70
RuS1·AuNP50	470	20	**RuS6·AuNP50**	340	40	**RuS12·AuNP50**	480	70
RuS1·AuNP100	470	20	**RuS6·AuNP100**	340	40	**RuS12·AuNP100**	480	70

To examine the effect of the Zonyl surfactant on the luminescence properties, we compared the luminescence decays of each ruthenium probe (RuS1, RuS6 and RuS12) upon addition of Zonyl (10 µL of 10% in water). Both the luminescence lifetimes of RuS6 and RuS12 increased upon addition of surfactant by 70% and 25% respectively, compared to the complex in solution (Figure 6f & g). In contrast, the lifetime of RuS1 did not change upon addition of Zonyl surfactant (Figure 6d). We attribute the increase in lifetime of RuS6 and RuS12 to interaction of the surfactant with the molecular complex and consequently protection from $^3O_2$ quenching. Increasing the hydrophobicity of a probe increases interaction with the surfactant and oxygen shielding allows for the largest change in luminescence lifetime upon addition of surfactant. Previous studies have shown that increasing hydrophobicity of the ligands increased ruthenium complex binding to ionic and non-ionic surfactants.[29-31] It was found that $Ru(phen)_2(CN)_2$ had a 10-fold increase in binding to the anionic sodium dodecyl sulfate surfactant when compared with the less hydrophobic $Ru(bpy)_2(CN)_2$ complex.[30] The lifetime increases significantly more for RuS6 (240 to 400 ns, 70%) than with RuS12 (280 to 350 ns, 25%) in the presence of Zonyl. This is attributed to a less tight interaction of RuS12 with Zonyl, possibly due to the presence of the amide bonds on the aliphatic legs. The lack of increase in lifetime for RuS1 may be attributed to the absence of aliphatic legs for the surfactant to interact with, deeming the complex more polar than RuS6 and RuS12.

To compare the effect of the different sized AuNP on the properties of the ruthenium probe we studied the luminescence lifetime decays for the isolated nanoparticles (AuNP13, AuNP50 and AuNP100) coated with ruthenium. The lifetime decays of RuS1·AuNP13, RuS1·AuNP50 and RuS1·AuNP100 overlap (Figure 6d), showing that there is no difference in the effect of size of AuNP on the luminescence lifetime of the probe (470 ns). Similar observations were made for the luminescence lifetime decays of RuS6·AuNP13, RuS6·AuNP50 and RuS6·AuNP100 (Figure 6e) as well as those of RuS12·AuNP13, RuS12·AuNP50 and RuS12·AuNP100 (Figure 6f). These results show that the size of the NP does not affect the luminescence lifetime of the three probes, RuS1, RuS6 and RuS12. It is worth noting here that for all the lifetime fittings of the coated AuNPs, we also observed a short component (50 – 100 ns) with small percentage contribution (5 – 20%). From our measurements this was attributed to be a scattering artifact and only the long component is reported.

The luminescence lifetimes of RuS1, RuS6 and RuS12 upon attachment to the AuNP showed an increase by 20%, 40% and 70% respectively from the free complex (Table 2). These results show that there is an enhancement of the lifetime from the Zonyl-coated AuNP surface, which can be attributed to the interaction with the Zonyl surfactant or to enhancement by AuNP surface. The enhancement of the RuS12 complex on the AuNP is significantly larger than that of RuS1 and RuS6, even though the effect of the Zonyl surfactant is less pronounced than in RuS6. This larger enhancement can be attributed to an interaction of the AuNP electromagnetic field with the luminescent probe dipole, observed only for RuS12 located at a longer distance from the particle surface than the other complexes. It is expected that the closer the luminescent probe is to the surface, the larger the quenching effect. This agrees with previous research which states that a lumophore close to the gold surface is quenched due to electronically interacting with the surface's strong magnetic field.[1] The effect is attributed to the excited electron being donated to the gold surface, quenching fluorescence by non-radiative pathways. In a study of a ruthenium complex with similar chain as the RuS6, a 60% quenching of luminescence was observed when attached to a gold surface.[19] In our case it is clear that the effect of Zonyl is important at this distance from the surface. It is also possible that the induced rigidity upon attachment of the ruthenium complexes to the surfactant functionalised AuNP contributes to the increase in luminescence lifetimes. Although there are examples of luminescence enhancement of lumophores on AuNP, most are at greater than 5 nm distances. No reports to our knowledge have been made of an enhancement in luminescence at these short distances from the surface. Estimated distances of the ruthenium centres in RuS1, RuS6 and RuS12 are 0.7, 1.6 and 2.5 nm from the surface respectively. Rubinstein *et al.* viewed a 4-fold increase in luminescence at a distance at 50 nm, but at 2 nm from the surface, which is equivalent to the RuS12 distance, they saw a large quenching in luminescence.[20] Our previous studies have shown that the luminescence lifetime of RuS12 is not quenched when the complex is attached to a gold surface, supporting the results that this distance is ideal for gold surfaces.[22] It is not surprising than for the AuNP, the enhancement can be observed at this distance based on the nanoparticle induced characteristics

Conclusions

We have demonstrated the effect of the distance of thiol-functionalised ruthenium complexes from the AuNP surface to the luminescence properties of the nanoparticles. The RuS12 complex is shown to display greater enhancement of luminescence upon attachment to AuNP which is significantly higher than those of RuS1 and RuS6 due to its improved distance from the gold surface. Even at these rather close distances to the gold surface, all three probes show an enhancement of luminescence lifetime when attached to the AuNP. We have shown that the coating with the Zonyl surfactant is important in the enhancement of the luminescence lifetime especially for the medium chain ruthenium complex.

The increase of the size of the AuNP from 13 to 50 and 100 nm led to probes with the same lifetimes as the 13 nm particles. Our studies provide an insight to the design of functionalised nanoparticles with luminescent probes which can be adopted for other fluorophores.

Experimental

Materials

Starting materials were purchased from Sigma Aldrich or Fisher Scientific.

Synthesis of Au NPs

AuNP13 The protocol for the formation of 13 nm Au NPs was based on a previous published method by Vossmeyer *et al*.[26] A solution of trisodium citrate dihydrate (60.3 mg, 0.21 mmol), citric acid (13.6 mg, 0.07 mmol) and ethylenediaminetetraacetic acid (EDTA) (1.6 mg, 0.004 mmol) in deionised water (100 mL) was vigorously stirred and brought to reflux. After 15 minutes of reflux, there was rapid addition of a preheated solution to 80 °C of gold(III) chloride trihydrate ($HAuCl_4.3H_2O$) (8.5 mg, 0.022 mmol) in deionised water (25 mL). After a further 15 minutes reflux, the heat was turned off and the solution was allowed to slowly cool to room temperature to form a 2 nM solution of AuNP13. λ_{max} (H_2O)/nm 517 (SPR). Diameter/nm = 14 ± 3 (DLS number distribution), PDI = 0.09. ζ-potential = - 46 ± 16 mV. To change the final concentration, AuNP13 were centrifuged at 13000 G for 30 minutes. The supernatant was decanted and the pellet was redispersed in deionised water to form a 9 nM solution of AuNP13.

AuNP50 and AuNP100 The protocol for the formation of AuNP50 and AuNP100 was modified using a previous published method by Ziegler *et al*.[24] Three stock solutions were prepared: 5 mM $HAuCl_4.3H_2O$; 57 mM ascorbic acid and 34 mM trisodium citrate dihydrate in water. AuNP13 (30 mL, 2 nM) were diluted to 40 mL with deionised water and vigorously stirred. The solutions for addition were diluted to 1 mM, 3 mM and 0.75 mM in deionised water for $HAuCl_4.3H_2O$, ascorbic acid and trisodium citrate dihydrate respectively. The two solutions ($HAuCl_4.3H_2O$ and ascorbic acid, trisodium citrate dihydrate) were simultaneously added *via* a peristaltic pump over 45 minutes. The resultant solution was refluxed for 30 minutes forming a solution of 0.7 nM AuNP25. λ_{max} (H_2O)/nm 520 (SPR). Diameter/nm = 24 ± 6 (DLS number distribution), PDI = 0.09. AuNP25 (9 mL, 0.7 nM) were diluted to 40 mL with deionised water and vigorously stirred. The solutions for addition were diluted to 1 mM, 3 mM and 0.75 mM in deionised water for $HAuCl_4.3H_2O$, ascorbic acid and trisodium citrate dihydrate respectively. The two solutions were simultaneously added *via* a peristaltic pump over 45 minutes. The resultant solution was refluxed for 30 minutes forming a solution of 80 pM AuNP50. λ_{max} (H_2O)/nm 532 (SPR). Diameter/nm = 50 ± 12 (DLS number distribution), PDI = 0.04. ζ-potential = - 31 ± 13 mV. AuNP50 was neutralised with 0.01 M NaOH solution. AuNP50 (40

mL, 80 pM) were vigorously stirred. The solutions for addition were diluted to 4 mM, 12 mM and 3.4 mM in deionised water for $HAuCl_4.3H_2O$, ascorbic acid and trisodium citrate dihydrate respectively. The two solutions were simultaneously added *via* a peristaltic pump over 45 minutes. The resultant solution was refluxed for 30 minutes forming a solution of 40 pM AuNP100. λ_{max} (H_2O)/nm 566 (SPR). Diameter/nm = 102 ± 24 (DLS number distribution), PDI = 0.01. ζ-potential = - 38 ± 12 mV. AuNP100 were taken and centrifuged at 13000 G for 90 s. The supernatant was decanted and the pellet was redispersed in deionised water.

Ruthenium molecular complexes

The RuS1, RuS6 and RuS12 probes were prepared using previously published methods and all characterisation agreed with previous results.[16, 22, 23] The counterion was exchanged using Dowex 1 X 8 ion exchange chromatography and the final solutions to be used for coating were prepared in methanol as 1.19, 0.95 and 0.87 mM solutions of RuS1, RuS6 and RuS12 respectively. RuS6 was sonicated with NH_4OH to produce a 0.63 mM solution.

Attachment of probe to NP

Z·AuNP13 10% Zonyl FSA solution in deionised water (10 µL) was added to 9 nM AuNP13 (1 mL) and sonicated for 10 mins. It was centrifuged at 13000 G for 30 mins, the supernatant was decanted and the pellet was resuspended in deionised water (1 mL) to form Z·AuNP13. λ_{max} (H_2O)/nm 518 (SPR). Diameter/nm = 12 ± 4 (DLS number distribution). ζ-potential = - 50 ± 8 mV.

RuS1·AuNP13 RuS1 (12 µL, 1.19 mM) was titrated into a 9 nM solution of Z·AuNP13 with sonication. A Sephadex G-10 size exclusion column was performed and the sample was diluted to 2 mL with deionised water to form a 4.5 nM solution of RuS1·AuNP13. λ_{max} (H_2O)/nm 521 (SPR). Diameter/nm = 15 ± 6 (DLS number distribution). ζ-potential = - 49 ± 11 mV. ICPMS result ratio Ru:Au is 1:180, suggesting 550 complexes per AuNP13.

RuS6·AuNP13 RuS6 (16 µL, 0.63 mM) was titrated into a 9 nM solution of Z·AuNP13 with sonication. A Sephadex G-10 size exclusion column was performed and the sample was diluted to 2 mL with deionised water to form a 4.5 nM solution of RuS6·AuNP13. λ_{max} (H_2O)/nm 522 (SPR). Diameter/nm = 24 ± 9 (DLS number distribution). ζ-potential = - 62 ± 15 mV. ICPMS result ratio Ru:Au is 1:180, suggesting 550 complexes per AuNP13.

RuS12·AuNP13 RuS12 (20 µL, 0.87 mM) was titrated into a 9 nM solution of Z·AuNP13 with sonication. A Sephadex G-10 size exclusion column was performed and the sample was diluted to 2 mL with deionised water to form a 4.5 nM solution of RuS12·AuNP13. λ_{max} (H_2O)/nm 520 (SPR). Diameter/nm = 18 ± 6 (DLS number distribution). ζ-potential = - 42 ± 13 mV. ICPMS result ratio Ru:Au is 1:150, suggesting 690 complexes per AuNP13.

Z·AuNP50 10% Zonyl FSA solution in deionised water (5 µL) was added to 80 pM AuNP50 (1 mL) and sonicated for 10 mins to form Z·AuNP50. λ_{max} (H_2O)/nm 533 (SPR). Diameter/nm = 50 ± 12 (DLS number distribution). ζ-potential = - 62 ± 18 mV.

RuS1·AuNP50 RuS1 (12 µL, 1.19 mM) was titrated into an 80 pM solution of Z·AuNP50 with sonication. A Sephadex G-10 size exclusion column was performed and the sample was diluted to 2 mL with deionised water to form a 40 pM solution of RuS1·AuNP50. λ_{max} (H_2O)/nm 537 (SPR). Diameter/nm = 59 ± 17 (DLS number distribution). ζ-potential = - 31 ± 10 mV.

RuS6·AuNP50 RuS6 (14 µL, 0.63 mM) was titrated into an 80 pM solution of Z·AuNP50 with sonication. A Sephadex G-10 size exclusion column was performed and the sample was diluted to 2 mL with deionised water to form a 40 pM solution of RuS6·AuNP50. λ_{max} (H_2O)/nm 536 (SPR). Diameter/nm = 54 ± 15 (DLS number distribution). ζ-potential = - 44 ± 16 mV.

RuS12·AuNP50 RuS12 (16 µL, 0.87 mM) was titrated into an 80 pM solution of Z·AuNP50 with sonication. A Sephadex G-10 size exclusion column was performed and the sample was diluted to 2 mL with deionised water to form a 40 pM solution of RuS12·AuNP50. λ_{max} (H_2O)/nm 537 (SPR). Diameter/nm = 61 ± 16 (DLS number distribution). ζ-potential = - 42 ± 12 mV.

Z·AuNP100 10% Zonyl FSA solution in deionised water (5 µL) was added to 40 pM AuNP100 (1 mL) and sonicated for 10 mins. It was centrifuged at 13000 G for 90 s, the supernatant was decanted and the pellet was resuspended in deionised water (1 mL) to form Z·AuNP100. λ_{max} (H_2O)/nm 567 (SPR). Diameter/nm = 107 ± 27 (DLS number distribution). ζ-potential = - 53 ± 11 mV.

RuS1·AuNP100 RuS1 (1 µL, 1.19 mM) was titrated into a 40 pM solution of Z·AuNP100 with sonication. A Sephadex G-10 size exclusion column was performed and the sample was diluted to 2 mL with deionised water to form a 20 pM solution of RuS1·AuNP100. λ_{max} (H_2O)/nm 569 (SPR). Diameter/nm = 109 ± 28 (DLS number distribution). ζ-potential = - 47 ± 10 mV.

RuS6·AuNP100 RuS6 (4 µL, 0.63 mM) was titrated into a 40 pM solution of Z·AuNP100 with sonication. A Sephadex G-10 size exclusion column was performed and the sample was diluted to 2 mL with deionised water to form a 20 pM solution of RuS6·AuNP100. λ_{max} (H_2O)/nm 569 (SPR). Diameter/nm = 107 ± 27 (DLS number distribution). ζ-potential = - 26 ± 9 mV.

RuS12·AuNP100 RuS12 (8 µL, 0.87 mM) was titrated into a 40 pM solution of Z·AuNP100 with sonication. A Sephadex G-10 size exclusion column was performed and the sample was diluted to 2 mL with deionised water to form a 20 pM solution of RuS12·AuNP100. λ_{max} (H_2O)/nm 569 (SPR). Diameter/nm = 112 ± 27 (DLS number distribution). ζ-potential = - 36 ± 10 mV.

Instrumentation

UV−vis spectroscopy was carried out on a Varian Cary 50 spectrophotometer. UV−vis spectra were collected using 1 cm path length quartz cuvettes. Luminescence spectroscopy was carried out on an Edinburgh Instruments FLS920 steady state and time-resolved spectrometer described elsewhere.[22] Luminescence lifetime experiments were carried out using an Edinburgh Instruments EPL-445 laser as the excitation source. Lifetimes were fitted using Edinburgh Instruments FAST software, with errors of ±10%. Luminescence experiments were carried out using 1 cm path length quartz cuvettes. TEM images were carried out on a Jeol 1200 EX transmission electron microscope. DLS sizing and zeta potential measurements were carried out on a Malvern Zetasizer nano ZSP and flow imaging was carried out on a Malvern Nanosight NS300.

Acknowledgments

We would like to thank John Ddungu for preliminary results. We wish to acknowledge EPSRC, The Leverhulme Trust (ZP) and the School of Chemistry, University of Birmingham for financial support. Some of the spectrometers used in this research were obtained through Birmingham Science City: Innovative Uses for Advanced Materials in the Modern World (West Midlands Centre for Advanced Materials Project 2), with support from Advantage West Midlands (AWM) and partial funding from the European Regional Development Fund (ERDF). We would like to thank Philip Aston at the University of Warwick for assistance with the ICPMS.

References

1. S. Eustis and M. A. El Sayed, *Chem. Soc. Rev.*, 2006, 35, 209-217.
2. E. Dulkeith, A. C. Morteani, T. Niedereichholz, T. A. Klar, J. Feldmann, S. A. Levi, F. C. J. M. van Veggel, D. N. Reinhoudt, M. Möller and D. I. Gittins, *Phys. Rev. Lett.*, 2002, 89, 203002.
3. K. G. Thomas and P. V. Kamat, *Acc. Chem. Res.*, 2003, 36, 888-898.
4. F. Liu and J. M. Nunzi, *Appl. Phys. Lett.*, 2011, 99, 123302.
5. J. Kümmerlen, A. Leitner, H. Brunner, F. R. Aussenegg and A. Wokaun, *Mol. Phys.*, 1993, 80, 1031-1046.
6. W. R. Glomm, S. J. Moses, M. K. Brennaman, J. M. Papanikolas and S. Franzen, *J. Phys. Chem. B*, 2004, 109, 804-810.
7. H. Zhang, M. Cao, W. Wu, H. Xu, S. Cheng and L.-J. Fan, *Nanoscale*, 2015, 7, 1374-1382.
8. A. V. Sorokin, A. A. Zabolotskii, N. V. Pereverzev, I. I. Bespalova, S. L. Yefimova, Y. V. Malyukin and A. I. Plekhanov, *J. Phys. Chem. C*, 2015, 119, 2743-2751.
9. I. O. Osorio-Román, A. R. Guerrero, P. Albella and R. F. Aroca, *Anal. Chem.*, 2014, 86, 10246-10251.
10. P. Reineck, D. Gómez, S. H. Ng, M. Karg, T. Bell, P. Mulvaney and U. Bach, *ACS Nano*, 2013, 7, 6636-6648.
11. N. S. Abadeer, M. R. Brennan, W. L. Wilson and C. J. Murphy, *ACS Nano*, 2014, 8, 8392-8406.

12. D. Lee and D. J. Jang, *Polymer*, 2014, 55, 5469-5476.
13. A. C. Savage and Z. Pikramenou, *Chem. Commun.*, 2011, 47, 6431-6433.
14. A. Davies, D. J. Lewis, S. P. Watson, S. G. Thomas and Z. Pikramenou, *Proc. Nat. Acad. Sci.*, 2012, 109, 1862-1867.
15. S. Comby, E. M. Surender, O. Kotova, L. K. Truman, J. K. Molloy and T. Gunnlaugsson, *Inorg. Chem.*, 2014, 53, 1867-1879.
16. N. J. Rogers, S. Claire, R. M. Harris, S. Farabi, G. Zikeli, I. B. Styles, N. J. Hodges and Z. Pikramenou, *Chem. Commun.*, 2014, 50, 617-619.
17. P. Zhang, J. Wang, H. Huang, H. Chen, R. Guan, Y. Chen, L. Ji and H. Chao, *Biomaterials*, 2014, 35, 9003-9011.
18. F. C. Leung, A. Y. Tam, V. K. Au, M.-J. Li and V. W. Yam, *ACS Appl. Mater. Interfaces*, 2014, 6, 6644-6653.
19. M. Jebb, P. K. Sudeep, P. Pramod, K. G. Thomas and P. V. Kamat, *J. Phys. Chem. B*, 2007, 111, 6839-6844.
20. O. Kedem, W. Wohlleben and I. Rubinstein, *Nanoscale*, 2014, 6, 15134-15143.
21. K. Wee, M. K. Brennaman, L. Alibabaei, B. H. Farnum, B. Sherman, A. M. Lapides and T. J. Meyer, *J. Am. Chem. Soc.*, 2014, 136, 13514-13517.
22. S. J. Adams, D. J. Lewis, J. A. Preece and Z. Pikramenou, *ACS Appl. Mater. Interfaces*, 2014, 6, 11598-11608.
23. P. Bertoncello, E. T. Kefalas, Z. Pikramenou, P. R. Unwin and R. J. Forster, *J. Phys. Chem. B*, 2006, 110, 10063-10069.
24. C. Ziegler and A. Eychmüller, *J. Phys. Chem. C*, 2011, 115, 4502-4506.
25. K. C. Grabar, R. G. Freeman, M. B. Hommer and M. J. Natan, *Anal. Chem.*, 1995, 67, 735-743.
26. F. Schulz, T. Homolka, N. G. Bastús, V. Puntes, H. Weller and T. Vossmeyer, *Langmuir*, 2014, 30, 10779-10784.
27. W. Haiss, N. T. K. Thanh, J. Aveyard and D. G. Fernig, *Anal. Chem.*, 2007, 79, 4215-4221.
28. S. K. Ghosh and T. Pal, *Chem. Rev.*, 2007, 107, 4797-4862.
29. B. Factor, B. Muegge, S. Workman, E. Bolton, J. Bos and M. M. Richter, *Anal. Chem.*, 2001, 73, 4621-4624.
30. S. W. Snyder, S. L. Buell, J. N. Demas and B. A. DeGraff, *J. Phys. Chem*, 1989, 93, 5265-5271.
31. W. J. Dressick, B. L. Hauenstein, T. B. Gilbert, J. N. Demas and B. A. DeGraff, *J. Phys. Chem*, 1984, 88, 3337-3340.